J|A|C|S
ARTICLES
Published on Web 05/07/2004

A Model for Describing the Thermodynamics of Multivalent Host−Guest Interactions at Interfaces

Jurriaan Huskens,* Alart Mulder, Tommaso Auletta, Christian A. Nijhuis, Manon J. W. Ludden, and David N. Reinhoudt

Contribution from the Laboratory of Supramolecular Chemistry and Technology, MESA+ Institute for Nanotechnology, University of Twente, P.O. Box 217, 7500 AE Enschede, The Netherlands

Received February 18, 2004; E-mail: j.huskens@utwente.nl

Abstract: A model has been described for interpreting the binding of multivalent molecules to interface-immobilized monovalent receptors through multiple, independent interactions. It is based on the concept of effective concentration, C_{eff}, which has been developed before for multivalent binding in solution and which incorporates effects of lengths and flexibilities of linkers between interacting sites. The model assumes: (i) the interactions are independent, (ii) the maximum number of interactions, p_{max}, is known, (iii) C_{eff} is estimated from (simple) molecular models. Simulations of the thermodynamics and kinetics of multivalent host−guest binding to interfaces have been discussed, and competition with a monovalent competitor in solution has been incorporated as well. The model was successfully used to describe the binding of a divalent guest to self-assembled monolayers of a cyclodextrin host. The adsorption data of more complex guest-functionalized dendrimers, for which p_{max} was not known beforehand, was interpreted as well. Finally, it has been shown that the model can aid to deconvolute contributions of multivalency and cooperativity to stability enhancements observed for the adsorption of multivalent molecules to interfaces.

Introduction

Multivalent interactions are of strong current interest, in particular in biochemistry.[1] They govern many interactions between proteins and small molecules, between proteins or antibodies and cell membranes, between viruses and cells, etc.[2] In particular, protein−carbohydrate interactions are intensively investigated, as they play a pivotal role in for example the binding of the influenza virus to cell membranes[3−6] and the recognition by carbohydrate-binding proteins (lectins)[7−14] which are essential in membrane recognition events, for which Concanavalin A often serves as a model system.[15−17] Their, often qualitative, understanding has led to the design of new inhibitors based on multivalency for example for cholera toxins and analogous systems.[18−20] For some systems, a thorough quantitative understanding has been obtained, e.g., for the multivalent binding to the pentavalent cholera toxins[21,22] and for the formation of a trivalent interaction between a trivalent peptide and a tris-vancomycin derivative.[23] In the latter case, it

(1) Mammen, M.; Choi, S.-K.; Whitesides, G. M. *Angew Chem., Int. Ed*. **1998**, *37*, 2754−2794.
(2) Varki, A. *Glycobiology* **1993**, *3*, 97−130.
(3) Matrosovich, M. N.; Mochalova, L. V.; Marinina, V. P.; Byramova, N. E.; Bovin, N. V. *FEBS Lett.* **1990**, *272*, 209−212.
(4) (a) Spaltenstein, A.; Whitesides, G. M. *J. Am. Chem. Soc.* **1991**, *113*, 686−687. (b) Lees, W. J.; Spaltenstein, A.; Kingery-Wood, J. E.; Whitesides, G. M. *J. Med. Chem.* **1994**, *37*, 3419−3433. (c) Sigal, G. B.; Mammen, M.; Dahmann, G.; Whitesides, G. M. *J. Am. Chem. Soc.* **1996**, *118*, 3789−3800. (d) Choi, S.-K.; Mammen, M.; Whitesides, G. M. *J. Am. Chem. Soc.* **1997**, *119*, 4103−4111.
(5) Glick, G. D.; Toogood, P. L.; Wiley, D. C.; Skehel, J. J.; Knowles, J. R. *J. Biol. Chem.* **1991**, *266*, 23660−23669.
(6) Sabesan, S.; Duus, J. Ø.; Neira, S.; Domaille, P.; Kelm, S.; Paulson, J. C.; Bock, K. *J. Am. Chem. Soc.* **1992**, *114*, 8363−8375.
(7) Lee, R. T.; Lin, P.; Lee, Y. C. *Biochemistry* **1984**, *23*, 4255−4261.
(8) DeFrees, S. A.; Kosch, W.; Way, W.; Paulson, J. C.; Sabesan, S.; Halcomb, R. L.; Huang, D.-H.; Ichikawa, Y.; Wong, C.-H. *J. Am. Chem. Soc.* **1995**, *117*, 66−79.
(9) Roy, R. *Curr. Opin. Struct. Biol.* **1996**, *6*, 692−702.
(10) MacKenzie, C. R.; Hirama, T.; Deng, S.; Bundle, D. R.; Narang, S. A.; Young, N. M. *J. Biol. Chem.* **1996**, *271*, 1527−1533.
(11) (a) Gestwicki, J. E.; Strong, L. E.; Kiessling, L. L. *Chem. Biol.* **2000**, *7*, 583−591. (b) Kiessling, L. L.; Gestwicki, J. E.; Strong, L. E. *Curr. Opin. Chem. Biol.* **2000**, *4*, 696−703. (c) Bertozzi, C. R.; Kiessling, L. L. *Science* **2001**, *291*, 2357−2364.
(12) Lundquist, J. J.; Toone, E. J. *Chem. Rev.* **2002**, *102*, 555−578.
(13) Vrasidas, I.; André, S.; Valentini, P.; Böck, C.; Lensch, M.; Kaltner, H.; Liskamp, R. M. J.; Gabius, H.-J.; Pieters, R. J. *Org. Biomol. Chem.* **2003**, *1*, 803−810.
(14) Kalovidouris, S. A.; Blixt, O.; Nelson, A.; Vidal, S.; Turnbull, W. B.; Paulson, J. C.; Stoddart, J. F. *J. Org. Chem.* **2003**, *68*, 8485−8493.
(15) (a) Kanai, M.; Mortell, K. H.; Kiessling, L. L. *J. Am. Chem. Soc.* **1997**, *119*, 9931−9932. (b) Cairo, C. W.; Gestwicki, J. E.; Kanai, M.; Kiessling, L. L. *J. Am. Chem. Soc.* **2002**, *124*, 1615−1619. (c) Gestwicki, J. E.; Cairo, C. W.; Strong, L. E.; Oetjen, K. A.; Kiessling, L. L. *J. Am. Chem. Soc.* **2002**, *124*, 14922−14933.
(16) Dam, T. K.; Roy, R.; Das, S. K.; Oscarson, S.; Brewer, C. F. *J. Biol. Chem.* **2000**, *275*, 14223−14230.
(17) Akai, S.; Kajihara, Y.; Nagashima, Y.; Kamei, M.; Arai, J.; Bito, M.; Sato, K. *J. Carbohydr. Chem.* **2001**, *20*, 121−143.
(18) Schön, A.; Freire, E. *Biochemistry* **1989**, *28*, 5019−5024.
(19) (a) Fan, E.; Zhang, Z.; Minke, W. E.; Hou, Z.; Verlinde, C. L. M. J.; Hol, W. G. J. *J. Am. Chem. Soc.* **2000**, *122*, 2663−2664. (b) Merrit, E. A.; Zhang, Z.; Pickens, J. C.; Ahn, M.; Hol, W. G. J.; Fan, E. *J. Am. Chem. Soc.* **2002**, *124*, 8818−8824. (c) Zhang, Z.; Merrit, E. A.; Ahn, M.; Roach, C.; Hou, Z.; Verlinde, C. L. M. J.; Hol, W. G.; Fan, E. J. *J. Am. Chem. Soc.* **2002**, *124*, 12991−12998.
(20) (a) Kitov, P. I.; Sadowska, J. M.; Mulvey, G.; Armstrong, G. D.; Ling, H.; Pannu, N. S.; Read, R. J.; Bundle, D. R. *Nature* **2000**, *403*, 669−672. (b) Kitov, P. I.; Shimizu, H.; Homans, S. W.; Bundle, D. R. *J. Am. Chem. Soc.* **2003**, *125*, 3284−3294.
(21) Gargano, J. M.; Ngo, T.; Kim, J. Y.; Acheson, D. W. K.; Lees, W. J. *J. Am. Chem. Soc.* **2001**, *123*, 12909−12910.
(22) Kitov, P. I.; Bundle, D. R. *J. Am. Chem. Soc.* **2003**, *125*, 16271−16284.
(23) (a) Rao, J.; Lahiri, J.; Isaacs, L.; Weis, R. M.; Whitesides, G. M. *Science* **1998**, *280*, 708−711. (b) Rao, J.; Lahiri, J.; Weis, R. M.; Whitesides, G. M. *J. Am. Chem. Soc.* **2000**, *122*, 2698−2710.

10.1021/ja049085k CCC: $27.50

has been proven that the employment of multiple interactions can lead to association and dissociation mechanisms which are fundamentally different from monovalent interactions.

Multivalent interactions at interfaces, e.g., at cell membranes,[24] at lipid membrane[25−27] or self-assembled monolayer (SAM)[28,29] model systems and at nanoparticles[30−32] and (polymer) vesicles,[33,34] are particularly important, though even less well understood, since such interfaces, when functionalized with monovalent receptors or ligands, can act as multivalent systems purely based on the immobilization of the monovalent agents at the interface. Concentrations of these agents at the interface can differ,[26−28a,c] and the distribution may be uneven and could even be altered upon binding with a multivalent counterpart.[24,26] Although often speculated upon, such effects have rarely been studied in a quantitative sense,[26] in large part because binding models incorporating multivalency effects at interfaces are lacking. Very recently, multivalency effects have been studied at the single molecule level by individually detecting the blocking of receptor pores in a lipid membrane.[35]

When multivalency is defined in a narrow sense, i.e., as an interaction, between two (or more) multivalent agents, which is constituted of multiple, *independent* interactions of the same motif, the thermodynamic interpretation of the combination of the multiple interactions is based on entropy terms.[1] Whether or not individual interactions can be regarded as independent can depend on spatial separation between receptor sites, linkers between ligand sites and between receptor sites, and their conformational degrees of freedom, and possibly on other factors. However, for a given multivalent system, it is often hard to judge whether interactions can be regarded as independent, and it should be preferentially supported by enthalpy data. Therefore, many interpretations are based on cooperativity,[26,27] i.e., a description of multivalent interactions allowing the change of individual interactions upon formation of preceding interactions. This, however, causes problems in finding a molecular understanding of the multivalent system, as the change in interaction strength has to be attributed to contributions from changes in conformations and internal interactions of receptors, ligands, and/or linkers, which are hard to dissect, let alone quantify. Additionally, traditional methods to experimentally verify extents of cooperativity, for example Hill and Scatchard plots, fail for multivalent systems, since they are only valid for the binding of multiple monovalent ligands to a multivalent receptor, as has been put forward most clearly by Ercolani.[36] In summary, a description based on cooperativity provides a way to fit a model to a given set of data and may allow a comparison to other systems, but the obtained model parameters only provide an (often misleading) sense of quantitative understanding in which the molecular picture often remains unclear.

A means to provide a molecular understanding of the way how multiple interactions can act together is to introduce the concept of effective concentration or molarity,[37] which can be seen as the concentration of an interacting, monovalent agent experienced by its counterpart as soon as one (or more) of the monovalent interactions have been formed. Effective molarity (EM) is based on relative formation rate constants between intra- and intermolecular steps for a formation of a given interaction or bond or, for reversible interactions, on the ratio between intra- and intermolecular complex stability constants. It has been applied to intramolecular reactions[37a,c,38] and even to the interpretation of reaction kinetics at SAMs.[39] It has also been applied to both reversible and irreversible macrocyclizations,[37b,40] including the assembly formation of, e.g., porphyrin complexes.[41−43] Effective concentration (C_{eff}), which has been shown to be conceptually close to or equal to effective molarity for various systems,[37c] is based on the probability with which two interacting sites can meet depending on the linker length, conformational possibilities, etc. between them.[44] The effective concentration can therefore be changed by changing linker lengths, which has been employed to probe distances between protein receptor sites[45] and to design the potentially most potent pentavalent inhibitors for the rigid cholera toxins.[21] It has also been successfully used in the interpretation of the kinetics of a divalent protein−antibody interaction.[46]

Another approach to deal with multivalency is to dissect the overall free energy into contributions stemming from inter- and intramolecular complexation steps, as was outlined by Jencks.[47] A stringent extrapolation of this methodology to explain the binding of synthetically prepared multivalent inhibitors to the

(24) Gestwicki, J. E.; Kiessling, L. L. *Nature* **2002**, *415*, 81−84.
(25) Pisarchik, M. L.; Thompson, N. L. *Biophys. J.* **1990**, *58*, 1235−1249.
(26) Doyle, E. L.; Hunter, C. A.; Phillips, H. C.; Webb, S. J.; Williams, N. H. *J. Am. Chem. Soc.* **2003**, *125*, 4593−4599.
(27) Yang, T.; Baryshnikova, O. K.; Mao, H.; Holden, M. A.; Cremer, P. S. *J. Am. Chem. Soc.* **2003**, *125*, 4779−4784.
(28) (a) Mann, D. A.; Kanai, M.; Maly, D. J.; Kiessling, L. L. *J. Am. Chem. Soc.* **1998**, *120*, 10575−10582. (b) Smith, E. A.; Thomas, W. D.; Kiessling, L. L.; Corn, R. M. *J. Am. Chem. Soc.* **2003**, *125*, 6140−6148.
(29) (a) Rao, J.; Yan, L.; Xu, B.; Whitesides, G. M. *J. Am. Chem. Soc.* **1999**, *121*, 2629−2630. (b) Rao, J.; Yan, L.; Lahiri, J.; Whitesides, G. M.; Weis, R. M.; Warren, H. S. *Chem. Biol.* **1999**, *6*, 353−359. (c) Horan, N.; Yan, L.; Isobe, H.; Whitesides, G. M.; Kahne, D. *Proc. Natl. Acad. Sci. U.S.A.* **1999**, *96*, 11782−11786. (d) Metallo, S. J.; Kane, R. S.; Holmlin, R. E.; Whitesides, G. M. *J. Am. Chem. Soc.* **2003**, *125*, 4534−4540.
(30) Liang, R.; Yan, L.; Loebach, J.; Ge, M.; Uozumi, Y.; Sekanina, K.; Horan, N.; Gildersleeve, J.; Thompson, C.; Smith, A.; Biswas, K.; Still, W. C.; Kahne, D. *Science* **1996**, *274*, 1520−1522.
(31) Barrientos, Á. G.; De la Fuente, J. M.; Rojas, T. C.; Fernández, A.; Penadés, S. *Chem.—Eur. J.* **2003**, *9*, 1909−1921.
(32) Lin, C.-C.; Yeh, Y.-C.; Yang, C.-Y.; Chen, G.-F.; Chen, Y.-C.; Wu, Y.-C.; Chen, C.-C. *Chem. Commun.* **2003**, 2920−2921.
(33) (a) Thibault, R. J., Jr.; Galow, T. H.; Turnberg, E. J.; Gray, M.; Hotchkiss, P. J.; Rotello, V. M. *J. Am. Chem. Soc.* **2002**, *124*, 15249−15254. (b) Thibault, R. J.; Hotchkiss, P. J.; Gray, M.; Rotello, V. M. *J. Am. Chem. Soc.* **2003**, *125*, 11249−11252.
(34) Ravoo, B. J.; Jacquier, J.-C.; Wenz, G. *Angew. Chem., Int. Ed.* **2003**, *42*, 2066−2070.
(35) Howorka, S.; Nam, J.; Bayley, H.; Kahne, D. *Angew. Chem., Int. Ed.* **2004**, *43*, 842−846.
(36) Ercolani, G. *J. Am. Chem. Soc.* **2003**, *125*, 16097−16103.
(37) For some reviews, see: (a) Kirby, A. J. *Adv. Phys. Org. Chem.* **1980**, *17*, 183−279. (b) Winnik, M. A. *Chem. Rev.* **1981**, *81*, 491−524. (c) Mandolini, L. *Adv. Phys. Org. Chem.* **1986**, *22*, 1−111.
(38) Mazor, M. H.; Wong, C. F.; McCammon, J. A.; Deutch, J. M.; Whitesides, G. *J. Phys. Chem.* **1990**, *94*, 3807−3812.
(39) Kumar, J. K.; Oliver, J. S. *J. Am. Chem. Soc.* **2002**, *124*, 11307−11314.
(40) (a) Roelens, S.; Dalla Cort, A.; Mandolini, L. *J. Org. Chem.* **1992**, *57*, 1472−1476. (b) Ercolani, G.; Mandolini, L.; Mencarelli, P.; Roelens, S. *J. Am. Chem. Soc.* **1993**, *115*, 3901−3908. (c) Ercolani, G. *J. Phys. Chem. B* **1998**, *102*, 5699−5703. (d) Galli, C.; Mandolini, L. *Eur. J. Org. Chem.* **2000**, 3117−3125.
(41) (a) Anderson, H. L. *Inorg. Chem.* **1994**, *33*, 972−981. (b) Anderson, H. L.; Anderson, S.; Sanders, J. K. M. *J. Chem. Soc., Perkin Trans. 1* **1995**, 2231−2245. (c) Anderson, S.; Anderson, H. L.; Sanders, J. K. M. *J. Chem. Soc., Perkin Trans. 1* **1995**, 2255−2267.
(42) (a) Chi, X.; Guerin, A. J.; Haycock, R. A.; Hunter, C. A.; Sarson, L. D. *J. Chem. Soc., Chem. Commun.* **1995**, 2563−2565. (b) Felluga, F.; Tecilla, P.; Hillier, L.; Hunter, C. A.; Licini, G.; Scrimin, P. *Chem. Commun.* **2000**, 1087−1088. (c) Baldini, L.; Ballester, P.; Casnati, A.; Gomila, R. M.; Hunter, C. A.; Sansone, F.; Ungaro, R. *J. Am. Chem. Soc.* **2003**, *125*, 14181−14189.
(43) (a) Ercolani, G.; Ioele, M.; Monti, D. *New J. Chem.* **2001**, *25*, 783−789. (b) Ercolani, G. *J. Phys. Chem. B* **2003**, *107*, 5052−5057.
(44) (a) Kuhn, W. *Kolloid-Z.* **1934**, *68*, 2−15. (b) Jacobson, H.; Stockmayer, W. H. *J. Chem. Phys.* **1950**, *18*, 1600−1606.
(45) Kramer, R. H.; Karpen, J. W. *Nature* **1998**, *395*, 710−713.
(46) Müller, K. M.; Arndt, K. M.; Plückthun, A. *Anal. Biochem.* **1998**, *261*, 149−158.
(47) Jencks, W. P. *Proc. Natl. Acad. Sci. U.S.A.* **1981**, *78*, 4046−4050.

Scheme 1. Equilibria Present in the Case of Binding of a Multivalent Guest G to Hosts H_s Immobilized at an Interface (Equilibria from Top to Bottom) and Incorporating Competition with a Monovalent Host H_l in Solution (Equilibria from Left to Right)

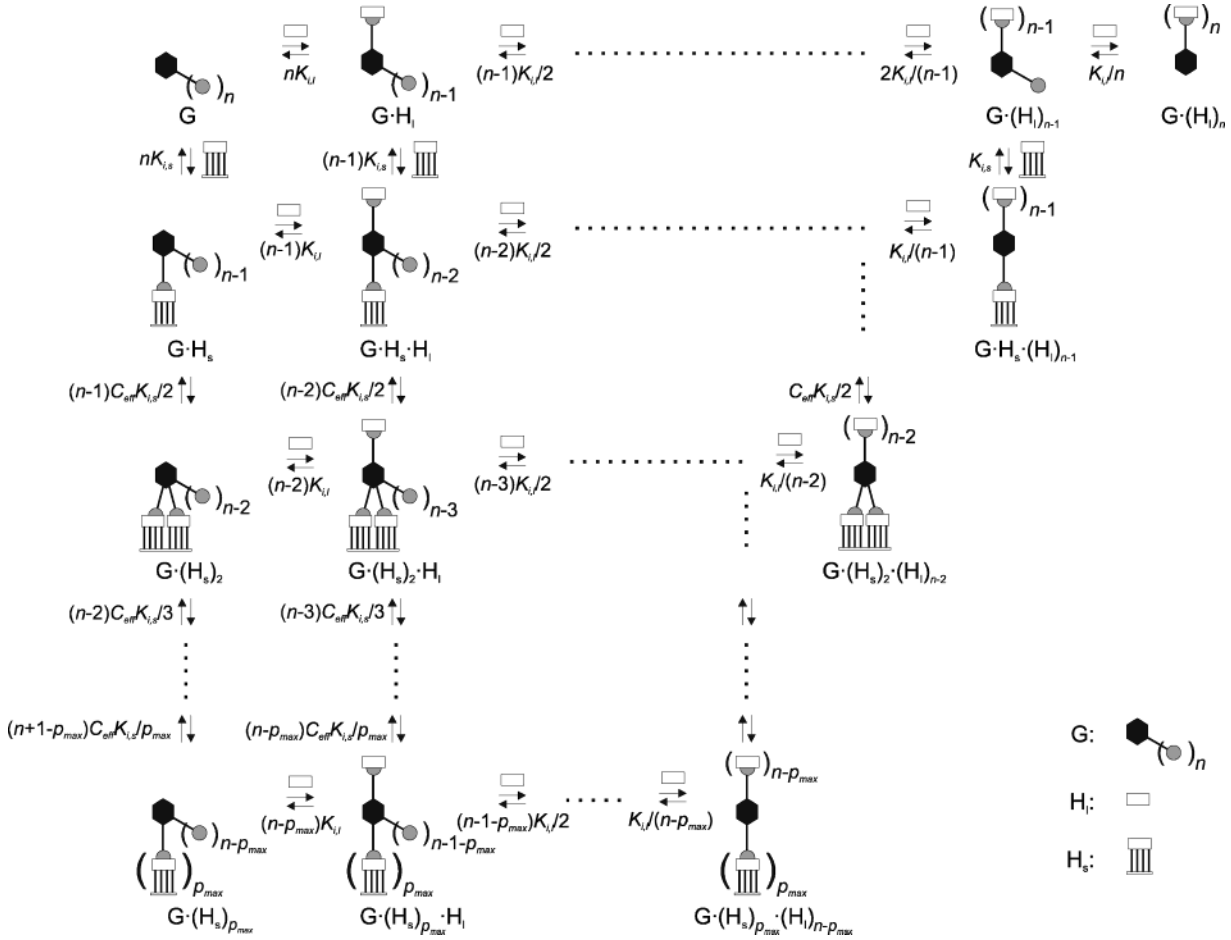

rigid cholera toxins was successfully followed recently by Kitov and Bundle.[22] However, linker lengths and molecular sizes of the ligands and receptors are not explicitly emerging from this model which makes it less readily applicable to the multivalent binding to immobilized *monovalent* receptors with varying surface concentrations, which is the main target of our study.

In this paper, the concept of effective concentration is employed in a model description of multivalent binding at interfaces. It can be used to describe the multivalent binding to two-dimensional ordered lattices of receptors, of which our recently developed molecular printboards form an excellent example,[48,49] as well as to disordered, randomly distributed receptor surfaces, possibly with varying coverages, as is the case for example in lipid membranes with receptors embedded.[26,27] The roles of linker lengths between interaction sites and receptor coverages are discussed in the framework of the effective concentration concept. It is shown how the model can be used to obtain intrinsic binding constants for individual interactions by fitting it to data obtained for multivalent systems with unambiguous numbers of interacting sites. The model can be used as well for determining the *number* of monovalent interactions for multivalent systems for which this number is less trivial, but the intrinsic binding constant can be safely assumed to be equal to values obtained for monovalent model compounds, as is the case for example for guest-functionalized dendrimers.[48,49] Furthermore, the implications for dissociation kinetics is briefly discussed as well.

Results and Discussion

Theoretical Model. The model that will be described below deals with the thermodynamics of the stepwise host−guest binding of multivalent guest molecules G, with n interaction sites for a host, to monovalent hosts H immobilized on a flat substrate (see Scheme 1).[50] Competition for guest binding with monovalent hosts in solution is also incorporated.[51] The binding constant of an individual interaction site of a guest with a host in solution ("liquid"), H_l, is governed by the intrinsic solution binding constant $K_{i,l}$ (= [guest site·H_l]/[guest site][H_l]), and the

(48) Huskens, J.; Deij, M. A.; Reinhoudt, D. N. *Angew. Chem., Int. Ed.* **2002**, *41*, 4467−4471.

(49) (a) Auletta, T.; Dordi, B.; Mulder, A.; Sartori, A.; Onclin, S.; Bruinink, C. M.; Nijhuis, C. A.; Beijleveld, H.; Péter, M.; Schönherr, H.; Vancso, G. J.; Casnati, A.; Ungaro, R.; Ravoo, B. J.; Huskens, J.; Reinhoudt, D. N. *Angew. Chem., Int. Ed.* **2004**, *43*, 369−373. (b) Mulder, A.; Auletta, T.; Sartori, A.; Del Ciotto, S.; Casnati, A.; Ungaro, R.; Huskens, J.; Reinhoudt, D. N. *J. Am. Chem. Soc.* **2004**, *126*, 6627−6636.

(50) Obviously, the host−guest terminology applied here is arbitrary, and the model can be applied as well to multivalent hosts binding to guest-functionalized SAMs, multivalent ligands binding to receptor interfaces, etc..

(51) Competition with a monovalent guest, to block free surface host sites, is fully symmetric, both regarding thermodynamics and kinetics, with competition with a monovalent host. This is made plausible by noting that the overall interaction is determined by monovalent interactions and that it is arbitrary which partner of such an interaction is occupied by a monovalent competitor. Therefore, the mathematics of this type of competition is not incorporated here but could be worked out analogously. The case given here, competition with a species which prevents adsorption of the multivalent analyte, is most common when data are collected based on surface coverages.

interaction with a host at the surface, H_s, is governed by the intrinsic surface binding constant $K_{i,s}$ (= [guest site·H_s]/[guest site][H_s]). All species are treated as solution species, i.e., calculated in volume concentrations, but surface concentrations (or coverages) of surface species can be easily derived from these. Besides the free species G, H_s, and H_l, complexes G·$(H_s)_p$·$(H_l)_q$ of stoichiometries 1:*p*:*q* are assumed to exist, where *p* ranges from 0 to p_{max} and *q* from 0 to $(n - p)$. The geometry and/or size of certain guest molecules may be such that only a maximum number of interactions, p_{max} ($\leq n$), can be formed to hosts at the surface, and obviously, the total number of bound guest sites ($p + q$) cannot exceed *n*. All species G, H_l, and G·$(H_l)_q$ (Scheme 1, top row) exist in solution, whereas species H_s and G·$(H_s)_p$·$(H_l)_q$ ($p \geq 1$) (Scheme 1, lower rows) are surface species.

The basic assumptions of the model are the following: (i) all individual host−guest interactions in solution, as well as on the surface, are treated equally, i.e., in absence of any form of (positive or negative) cooperativity, and (ii) the sequential binding steps of guest sites of surface-attached species to neighboring free surface host sites can be described using an effective concentration parameter, C_{eff}, which is assumed independent of the number of binding sites of the guest but only dependent on the molecular geometry (linker length, stiffness, etc.) of the guest and the number of hosts that a nonattached guest site can reach at the surface (see below).

In principle, such a model can be regarded as an entropy model as the enthalpic contributions of the individual interactions are simply summed when dealing with multivalent binding,[1] while all factors related to the nature of the combination of the multiple interactions are incorporated in the entropy term. For clarity, especially when dealing with systems for which the binding stoichiometry is unclear beforehand (see below), and for reasons of argument, because enthalpic and entropic contributions to the binding strengths can rarely be determined for surface-confined host−guest systems, we chose to set up the model in stability constant terminology, as commonly employed for simple host−guest equilibria but also, for example, for more complex assemblies.[42c,52]

The mass balances for the total concentrations of G, H_s, and H_l are given in eqs 1−3.

$$[G]_{tot} = \sum_{p=0}^{p_{max}(n-p)} \sum_{q=0} [G\cdot(H_s)_p\cdot(H_l)_q] \quad (1)$$

$$[H_s]_{tot} = [H_s] + \sum_{p=1}^{p_{max}(n-p)} \sum_{q=0} p[G\cdot(H_s)_p\cdot(H_l)_q] \quad (2)$$

$$[H_l]_{tot} = [H_l] + \sum_{p=0}^{p_{max}(n-p)} \sum_{q=1} q[G\cdot(H_s)_p\cdot(H_l)_q] \quad (3)$$

As mentioned above, an individual interaction between a guest site and a host H_l is governed by the intrinsic stability constant $K_{i,l}$. Concentrations of complexes in solution for the sequential binding events of hosts H_l to a multivalent guest G (thus for the equilibria: $G\cdot(H_l)_{q-1} + H_l \leftrightarrow G\cdot(H_l)_q$, valid for $q = 1..n$, Scheme 1, top row) can therefore, in the absence of cooperativity, be described by eq 4.

$$[G\cdot(H_l)_q] = \frac{(n - q + 1)}{q} K_{i,l}[G\cdot(H_l)_{q-1}][H_l] \quad (4)$$

In an analogous manner, the binding of a molecule G to a surface host, H_s, with a single interaction is described by eq 5.

$$[G\cdot H_s] = nK_{i,s}[G][H_s] \quad (5)$$

The binding events of sequential guest sites to other free surface hosts, $G\cdot(H_s)_{p-1} + H_s \leftrightarrow G\cdot(H_s)_p$ (for $p = 2..p_{max}$, Scheme 1, left column), are then described by eq 6.

$$[G\cdot(H_s)_p] = \frac{(n - p + 1)}{p} K_{i,s}[G\cdot(H_s)_{p-1}]C_{eff} \quad (6)$$

Compared to eqs 4 and 5, the expected $[H_s]$ has been replaced by the effective concentration, C_{eff}, i.e., the concentration of accessible, unbound H_s sites in the volume that can be probed by the interacting guest site (see below). The effective concentration is surface-coverage dependent, according to eq 7, since the concentration of accessible H_s sites in the probing volume, $C_{eff,max}$, which is the maximum, limiting value reached at infinitely low surface coverages, has to be multiplied by the fractional coverage, θ_f (= $[H_s]/[H_s]_{tot}$), of free surface hosts H_s, to obtain the concentration of accessible, unbound H_s sites in this probing volume.

$$C_{eff} = C_{eff,max}\theta_f = C_{eff,max}\frac{[H_s]}{[H_s]_{tot}} \quad (7)$$

Sequential binding events of hosts H_l from solution to these surface-attached species, according to $G\cdot(H_s)_p\cdot(H_l)_{q-1} + H_l \leftrightarrow G\cdot(H_s)_p\cdot(H_l)_q$ valid for $q = 1..(n - p)$, can be described, analogous to eq 4, by eq 8, where it has to be kept in mind that the number of guest sites available for interaction with H_l is $(n - p)$ instead of *n*.

$$[G\cdot(H_s)_p\cdot(H_l)_q] = \frac{(n - p - q + 1)}{q} K_{i,l}[G\cdot(H_s)_p\cdot(H_l)_{q-1}][H_l] \quad (8)$$

The total volume concentration of surface hosts, $[H_s]_{tot}$, can be calculated from the total surface area, A_s, the coverage, Γ_s, of hosts at the surface (in mol per surface area), and the sample volume, *V*, according to eq 9.

$$[H_s]_{tot} = \frac{\Gamma_s A_s}{V} \quad (9)$$

In a simulation or fit to experimental data, a complete speciation is obtained, and thus, the contribution of each individual species can be made visible. Some important concentrations or parameters, as will be used below, can be obtained from these. The total guest concentration at the surface, $[G]_s$, is given by eq 10.

$$[G]_s = \sum_{p=1}^{p_{max}(n-p)} \sum_{q=0} [G\cdot(H_s)_p\cdot(H_l)_q] \quad (10)$$

(52) For example, see: (a) Perlmutter-Hayman, B. *Acc. Chem. Res.* **1986**, *19*, 90−96. (b) Taylor, P. N.; Anderson, H. L. *J. Am. Chem. Soc.* **1999**, *121*, 11538−11545. (c) Bielejewska, A. G.; Marjo, C. E.; Prins, L. J.; Timmerman, P.; De Jong, F.; Reinhoudt, D. N. *J. Am. Chem. Soc.* **2001**, *123*, 7518−7533.

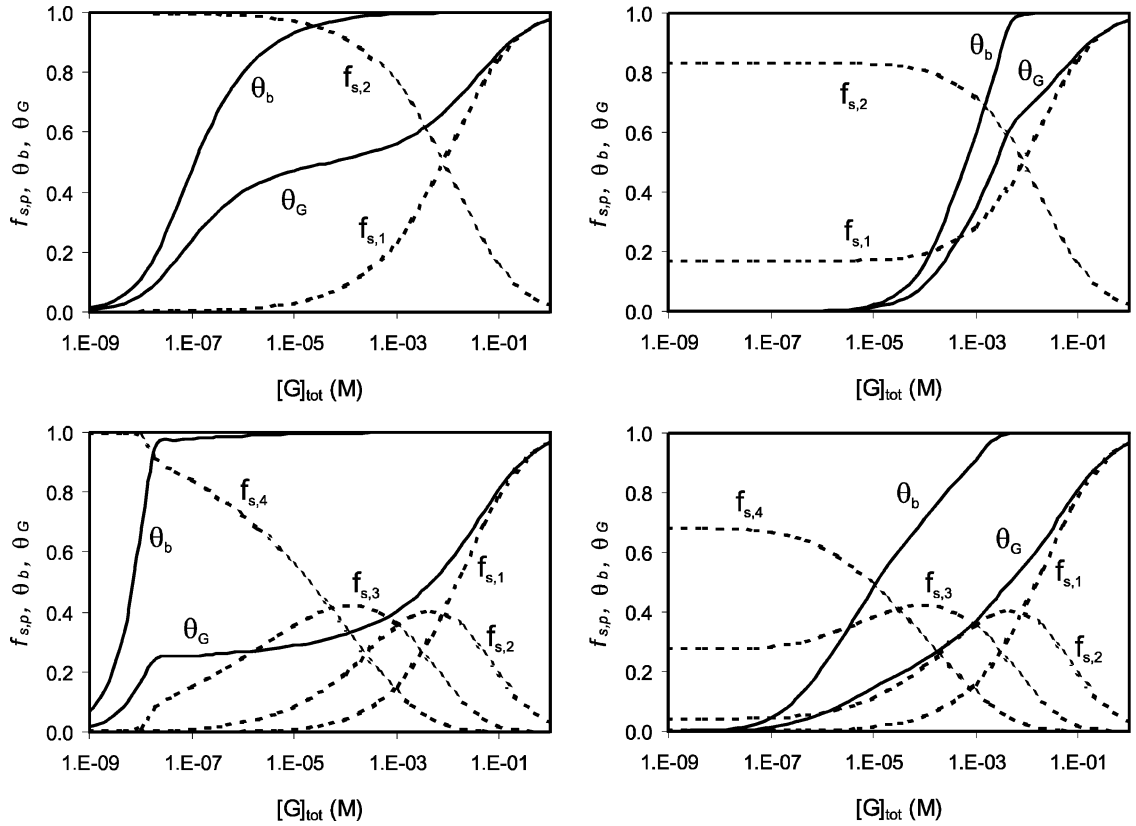

Figure 1. Simulated host (θ_b) and guest (θ_G) coverages and fractions $f_{s,p}$ of guest attached to the surface with p interactions (using $C_{eff,max} = 0.1$ M, $\Gamma_s = 6.0 \times 10^{-11}$ mol cm^{-2}, $K_{i,s} = K_{i,l} = 10^4$ M^{-1}) for $n = p_{max} = 2$ (top), $n = p_{max} = 4$ (bottom), $[H_l]_{tot} = 0$ (left), $[H_l]_{tot} = 0.01$ M (right).

The total guest concentration in solution, $[G]_l$, is given by eq 11, so that $[G]_{tot} = [G]_s + [G]_l$.

$$[G]_l = \sum_{q=0}^{n} [G{\cdot}(H_l)_q] \tag{11}$$

The concentration of guest species bound to the surface by a specific number of interactions, p, is given by eq 12, and the fraction of bound guest species with this number of interactions, $f_{s,p}$, is given by eq 13.

$$[G]_{s,p} = \sum_{q=0}^{(n-p)} [G{\cdot}(H_s)_p{\cdot}(H_l)_q] \tag{12}$$

$$f_{s,p} = \frac{[G]_{s,p}}{[G]_s} \tag{13}$$

The average number, p_{av}, of interactions used by a guest molecule to bind to the surface is equal to the concentration ratio of occupied surface sites and adsorbed guest and is given by eq 14.

$$p_{av} = \frac{[H_s]_{tot} - [H_s]}{[G]_s} = \sum_{p=1}^{p_{max}} p\frac{[G]_{s,p}}{[G]_s} = \sum_{p=1}^{p_{max}} p f_{s,p} \tag{14}$$

Other important surface-related parameters are the coverages of surface sites θ_f ($= [H_s]/[H_s]_{tot}$) and θ_b ($= 1 - \theta_f$) for the free and bound H_s sites, respectively, and the guest coverage θ_G ($= [G]_s/[H_s]_{tot}$), which is equal to θ_b/p_{av}.

In a numerical routine, using a Simplex algorithm, concentrations of all complexes are calculated from initial estimates for $[G]$, $[H_s]$, and $[H_l]$, and errors between calculated and experimental mass balances are minimized by optimizing these concentrations in an iterative process, as has been described before.[53]

Thus, simulations can be performed as shown in Figure 1, in which characteristic coverages θ_b and θ_G are given, as well as the fractions, $f_{s,p}$, of guest bound to the surface with 1 to n interactions, as a function of guest concentration in solution. The top two graphs show results for $n = 2$ and the bottom two for $n = 4$. The left two graphs have been obtained in the absence of monovalent competing hosts in solution, and the right two graphs, in the presence of a high concentration of competitor.

Without competitor (left two graphs), the simulations show that two distinct regimes are present. At relatively low $[G]_{tot}$, the guest adsorbs with the highest possible number of interactions ($f_{s,n} = 1$; here only simulations with $p_{max} = n$ are shown) until the coverage of bound host, θ_b, approaches 1. In this part, obviously, $\theta_G = \theta_b/n$. In this regime, the simulations show a Langmuir-type adsorption behavior, and this is the concentration range normally employed experimentally when evaluating stability constants. The comparison between $n = 2$ (top left graph) and $n = 4$ (bottom left) shows that full occupation of the surface sites is reached, as expected, at lower $[G]_{tot}$ for higher n. In the second regime, at higher $[G]_{tot}$, θ_G starts to rise further (deviating from Langmuirian behavior, but only detectible when employing a technique with which θ_G is measured rather than θ_b; see below), while all surface sites have been and remain

(53) Huskens, J.; Van Bekkum, H.; Peters, J. A. *Comput. Chem.* **1995**, *19*, 409−416.

bound, thus necessarily with a concomitant decrease of p_{av}. This is visible in the decrease of $f_{s,n}$ and the increase of $f_{s,p}$ with $p < n$. Only at very high $[G]_{tot}$, all of the guest is bound through only one interaction (θ_G and $f_{s,1} \rightarrow 1$).

The right two graphs show simulations of guest adsorption in the presence of a constant, high concentration of competing monovalent host in solution. It can be seen that, already at low $[G]_{tot}$, the guest adsorbs with less than the maximum number of interactions, and that there is no clear distinction anymore between the two regimes as was found in the absence of competitor. At intermediate, increasing levels of competitor, the occupation of surface host sites occurs at higher $[G]_{tot}$, thus effectively merging the first regime into the unchanging second regime. The behavior at high competitor concentrations, as shown in the two right graphs, clearly shows an overall non-Langmuirian adsorption behavior with a continually decreasing p_{av}. When experimental data are obtained at fairly low $[G]_{tot}$, such non-Langmuirian behavior is not necessarily visible from the experimental graph (as is seen in some systems as discussed below) but may only become apparent when measuring at large ranges of $[G]_{tot}$ or when fitting the data to a multivalency model, such as presented here.

Fitting the Model to Experimental Data. The use of the multivalency model described here to fit experimental data depends on the type of coverage data obtained. When the data provide coverages based on the amount of adsorbed (guest) molecules, as is the case in fitting SPR data (see below), it is assumed that the measured quantity, e.g., SPR angle, changes linearly with the concentration of guest species at the surface, $[G]_s$, irrespective of the number of interactions involved in binding these guest species to the surface. The fitting of, for example, SPR angle changes, $\Delta\alpha$, is performed according to eq 15.

$$\Delta\alpha = \frac{[G]_s}{[H_s]_{tot}}\Delta\alpha_{max} = \theta_G\Delta\alpha_{max} = \theta_b\frac{\Delta\alpha_{max}}{p_{av}} \qquad (15)$$

Here, $\Delta\alpha_{max}$ is a fit parameter corresponding to the maximal angle change expected for a fully covered surface at which each guest is bound by only one interaction, and the use of the guest coverage θ_G ($= [G]_s/[H_s]_{tot}$) ensures that the fitted $\Delta\alpha_{max}$ values are independent of sample volume. In principle, p_{av} is also coverage-dependent, but often it can be assumed that $p_{av} = p_{max}$ (see below) so that $\Delta\alpha$ is linearly dependent on the coverage of the surface-attached host sites, θ_b. Nevertheless, in principle this type of experiments can provide information on (possibly changing) numbers of interacting sites.

When experimental data directly provide coverages based on free/occupied surface (host) sites, for example, when using changing fluorescence intensities, ΔI, of surface-attached, fluorescently labeled receptors, intensities can be fitted using eq 16.

$$\Delta I = \theta_b\Delta I_{max} \qquad (16)$$

Here, ΔI_{max} is the maximal intensity change which is reached at full coverage of all surface-attached host sites. In this case, once all host sites have been bound, no additional information on numbers of interacting sites, which could change when more guest molecules bind thus necessarily lowering p_{av}, can be obtained.

Typically, in a least squares optimization routine, the sum of the squares of the differences between calculated and experimental $\Delta\alpha$ (or ΔI) values are minimized while changing $K_{i,s}$ and $\Delta\alpha_{max}$ (ΔI_{max}). Other parameters such as the maximum number of interactions, p_{max}, the maximum effective concentration, $C_{eff,max}$, and the intrinsic binding constant in solution, $K_{i,l}$, are either assumed known, estimated from molecular geometries, or determined from independent experiments. This methodology is, therefore, principally suited to determine the (intrinsic) binding constant of guests at surfaces covered with hosts.[50] Nevertheless, the procedure shown here can also be used to determine p_{max} when good estimates of $C_{eff,max}$ and $K_{i,s}$ exist, as will be outlined below.

The model described here incorporates effects of competition by the addition of a competing, monovalent host in solution. In principle, the model could be expanded to incorporate the occurrence of different guests and/or hosts in solution and/or at the surface, of multivalent hosts in solution, etc.. It only would require adaptation of the mass balance equations and the incorporation of the complex stoichiometries and/or stabilities into the intrinsic binding constant description shown above. Since we will describe comparisons to experimental data only in cases with one type of guest and competition for its binding between monovalent hosts in solution and at the surface, such descriptions will not be elaborated on any further here.

Effective Concentration. The effective concentration parameter, $C_{eff,max}$, is essential to the model described here. It represents the concentration of (free, uncomplexed) surface host sites H_s felt by a noncomplexed guest site connected to a surface-bound guest site by a linker of length L in the probing volume, $v(L)$, probed by this noncomplexed site. In general, for example for macrocyclizations, the effective concentration is defined as the probability with which polymer endgroups meet and is based on polymer random walk statistics.[37] Crucial are the structure, length, and behavior of the linker.

In principle, the probability with which an additional guest site could reach another surface host site can be calculated, as has been done for rigid receptors with well-defined inter-receptor distances in solution,[21] and optimal linker lengths can be determined by molecular modeling.[20] However, such calculations only work for fairly long chain lengths, since they are based on the limit for infinite polymer lengths, in which case also estimation of the stiffnesses of the linkers becomes possible. For small molecules, as are used in the systems shown below, such a calculation would become inaccurate. Furthermore, on the type of surfaces discussed here, there are no well-defined inter-receptor distances, but rather an infinite, continuous range of distances or at best (for perfectly hexagonally packed receptor interfaces) infinite numbers of discrete distances with different numbers of receptors corresponding to them. Therefore, we chose to approximate linker lengths from their maximal extension, which can often be easily estimated from molecular mechanics or even CPK models, and to define the probing volume at the interface as a half sphere with radius L, so $v(L) = (^2/_3)\pi L^3$. Assuming that, besides the one H_s unit used for binding one guest site, the remaining hosts H_s are free for binding, $C_{eff,max}$ is given by eq 17, in which $n_H(L)$ is the linker length-dependent number of accessible host sites in the probing

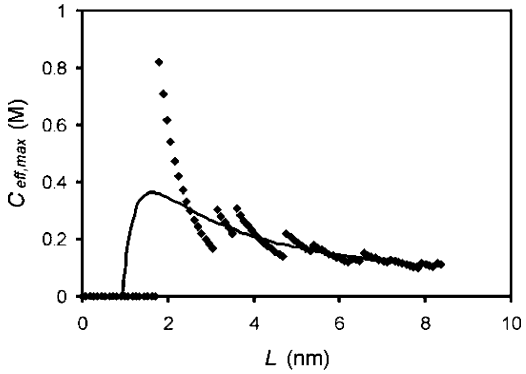

Figure 2. Predicted effective molarities, $C_{eff,max}$, of surface host sites experienced by an uncomplexed guest site of a multivalent guest connected to a host surface through a bound guest site with linker length, L, for a hexagonally ordered host lattice with a periodicity, a, of 1.8 nm (markers) or a disordered host lattice with the same density of host sites (line).

volume and N_{Av} is Avogadro's number.

$$C_{eff,max} = \frac{n_H(L)}{N_{Av}v(L)} = \frac{n_H(L)}{(^2/_3)\pi N_{Av}L^3} \quad (17)$$

In a perfectly hexagonal lattice of hosts with lattice parameter, a, $n_H(L)$ will show a discrete dependence on L as the number of accessible hosts increases from 0 (for $L/a < 1$) to 6 (for $1 \le L/a < \sqrt{3}$), to 12 (for $\sqrt{3} \le L/a < 2$), to 18 (for $2 \le L/a < \sqrt{7}$), etc.. This is reflected in $C_{eff,max}$, as is shown in Figure 2, in which the markers show this discrete behavior as calculated for a lattice parameter of 1.8 nm (used below for describing the data obtained for the cyclodextrin SAMs[54]). Alternatively, $n_H(L)$ can be approximated by the average number of hosts in the probing volume, which is equal to $\pi L^2 N_{Av}\Gamma_s$ where Γ_s is the surface coverage of host sites (in mol per surface area), while subtracting the one complexed host site. Thus, eq 17 is reduced to eq 18.

$$C_{eff,max} = \frac{\pi L^2 N_{Av}\Gamma_s - 1}{(^2/_3)\pi N_{Av}L^3} \quad (18)$$

For proper comparison, it has to be noted that, for geometry reasons, the coverage Γ_s is connected to the lattice parameter a by eq 19.

$$\Gamma_s = \frac{2}{\sqrt{3}N_{Av}a^2} \quad (19)$$

$C_{eff,max}$ calculated as a function of L using eqs 18 and 19, also for $a = 1.8$ nm ($\Gamma_s = 6.0 \times 10^{-11}$ mol cm^{-2}),[55] is shown in the continuous curve in Figure 2. Most likely, the latter way of estimating $C_{eff,max}$ is more appropriate for disordered host lattices with comparable surface densities and, thus, for example, for membrane-bound receptors. The comparison between the two methods shows that large deviations of $C_{eff,max}$ between ordered and disordered lattices will be only apparent for $0.5 < L/a < 1.7$. Only in this range, one could expect maybe even experimentally accessible dependencies on lattice order, while for larger linkers ($L/a > 1.7$), the relative differences in $C_{eff,max}$ become rapidly negligible, and eq 18 can be reduced to eq 20 (also disregarding the one occupied host site), in which it is shown that $C_{eff,max}$ scales with L^{-1}.

$$C_{eff,max} = \frac{\pi L^2 N_{Av}\Gamma_s}{(^2/_3)\pi N_{Av}L^3} = \frac{3\Gamma_s}{2L} \quad (20)$$

Furthermore, it is clear from Figure 2 that, for a large range of synthetically available linkers and definitely for the molecules studied here (see Chart 1), $C_{eff,max}$ is expected to be in the range of 0.1−0.4 M (for an interface fully covered with hosts).

Since optimized $K_{i,s}$ values normally show a dependence on $C_{eff,max}$ of $C_{eff,max}{}^{-x}$ (with $x = (p_{max} - 1)/p_{max}$; see below), the relatively wide $C_{eff,max}$ range is predicted to have only a marginal influence on the optimized $K_{i,s}$ values, often within the experimental error. This fact, in addition to the reasons mentioned above, eliminates the need for sophisticated modeling of the linker lengths and molecular geometries to estimate $C_{eff,max}$; in many cases, a simple CPK model will suffice. On the other hand, the calculation shown here does not incorporate effects of inaccessible volume caused by the linker and other guest sites in the probing volume, surface roughness, and other effects, and the model shown above does not incorporate changes in $C_{eff,max}$ that may occur for subsequent host−guest interactions because of restrictions to molecular motion when two or more guest sites are bound. Consequently, only one $C_{eff,max}$ value is used for one particular guest molecule, also for the multivalent dendrimer molecules (**3a** and **3b**; see Chart 1).

Determination of the Intrinsic Binding Constant at the Surface, $K_{i,s}$. Cyclodextrin (CD) (**1a**, Chart 1) can act as a host for the binding of a variety of small, organic guest functionalities in water through hydrophobic interactions.[56] All experimental results discussed below as a comparison to the model's predictions were obtained with SAMs of the CD heptakis-(thioether) derivative **1b** (Chart 1) on gold as the host surfaces, as described before.[57,58] Such adsorbates form densely packed, well-ordered SAMs with equivalent binding sites, the near-hexagonal packing of which has been visualized by AFM.[58] Binding of small, univalent guest molecules to these SAMs has been studied by surface plasmon resonance (SPR)[59] and electrochemical impedance spectroscopies (EIS),[58] and an important finding was that the interaction strengths of such guest molecules with CDs on the SAMs are identical to the binding strengths in solution.[59] The binding of large, adamantyl- (Ad-) functionalized dendrimers employing multiple interactions has recently been discussed as well.[48] This has led to the development of so-called molecular printboards to which molecules can be bound strongly but reversibly using multiple interactions, as

(54) This periodicity corresponds to an occupation of 2.8 nm^2 per CD cavity which arises from 14 alkyl chains closely packed below the cavity, each occupying 0.2 nm^2.

(55) The surface coverage representing the surface concentration at the nm level is $\Gamma_s = 6.0 \times 10^{-11}$ mol cm^{-2} as calculated from a lattice periodicity of 1.8 nm. In practice, the macroscopic surface coverage is somewhat higher ($\Gamma_s = 7.9 \times 10^{-11}$ mol cm^{-2}), as determined independently from the SPR binding data of **2a** (for $[H_I]_{tot} = 0.1$ mM, Figure 3) and electrochemistry data obtained for **3a** and **3b** (see ref 66). The difference (factor 1.3) is attributed to the surface roughness of the samples.

(56) Szejtli, J. *Comprehensive Supramolecular Chemistry*, *Vol. 3*; Pergamon: Oxford, 1996, and references therein.

(57) Beulen, M. W. J.; Bügler, J.; Lammerink, B.; Geurts, F. A. J.; Biemond, E. M. E. F.; Van Leerdam, K. G. C.; Van Veggel, F. C. J. M.; Engbersen, J. F. J.; Reinhoudt, D. N. *Langmuir* **1998**, *14*, 6424−6429.

(58) Beulen, M. W. J.; Bügler, J.; De Jong, M. R.; Lammerink, B.; Huskens, J.; Schönherr, H.; Vancso, G. J.; Boukamp, B. A.; Wieder, H.; Offenhäuser, A.; Knoll, W.; Van Veggel, F. C. J. M.; Reinhoudt, D. N. *Chem.—Eur. J.* **2000**, *6*, 1176−1183.

(59) De Jong, M. R.; Huskens, J.; Reinhoudt, D. N. *Chem.—Eur. J.* **2001**, *7*, 4164−4170.

Chart 1. Host (**1a**, **1b**) and Guest Molecules (**2a**, **2b**, **3a**, **3b**) Used in This Study

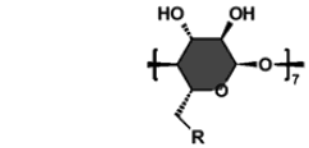

1a R = OH
1b R = $NH(CO)(CH_2)_{11}S(CH_2)_{11}CH_3$

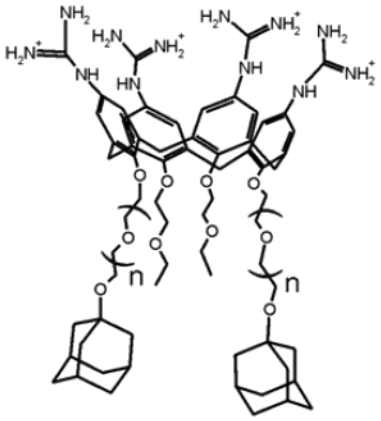

2a n = 3
2b n = 1

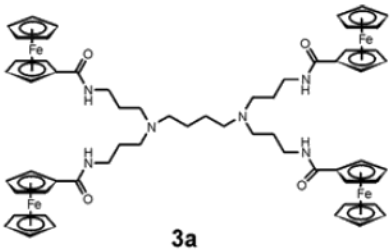

3a

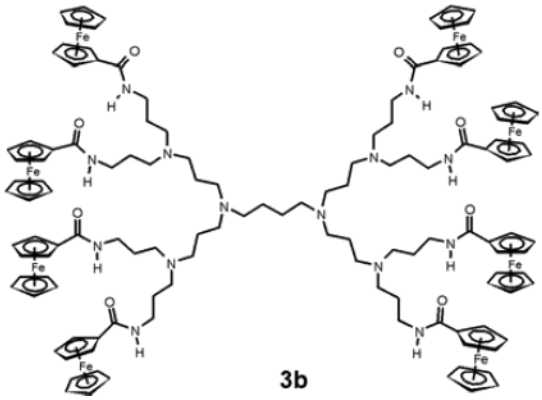

3b

has been shown for the transfer of molecules to such printboards using supramolecular microcontact printing and dip-pen nanolithography.[49]

The binding of the water-soluble calix[4]arene **2a** (Chart 1), containing two Ad moieties as the guest motif, with CD in solution and onto CD SAMs has been investigated by microcalorimetry and SPR, respectively.[49] The binding behavior to CD in water showed an independent binding of the two Ad groups, involving a CD for each Ad with binding parameters characteristic of Ad-β-CD interactions. The binding constant K obtained for this guest with a CD dimer in solution (1.2×10^7 M^{-1}) has been successfully interpreted using the effective concentration concept.[49] From molecular modeling it was estimated that C_{eff} was in this case approximately 3 mM.

The interaction of **2a** with the CD SAMs appeared to be much stronger: a Langmuir fit to data without a competing host in solution gave an apparent binding constant of 10^9-10^{11} M^{-1}.[49] The much higher apparent binding constant compared to the solution value was ascribed to the higher local concentration of hosts at the surface, i.e., to a higher C_{eff} value.

When adopting the model outlined above, $n = 2$ follows from the molecular structure of the guest (G) **2a**. Molecular modeling shows that the linker is long enough for both Ad groups to interact with the surface ($p_{max} = 2$) and that $C_{eff,max}$ is approximately 0.2 M (disregarding possible effects of hexagonal packing of the CD host lattice). $K_{i,l}$ ($= 4.6 \times 10^4$ M^{-1}) is known from microcalorimetry data of **2a**[49] and is similar to values obtained before for mono-Ad derivatives.[59] Therefore, the model contains the following species: G (= **2a**), H_l (= CD (**1a**) in solution), $G{\cdot}H_l$, and $G{\cdot}(H_l)_2$ in solution and H_s (= **1b** at a CD SAM), $G{\cdot}H_s$, $G{\cdot}H_s{\cdot}H_l$, and $G{\cdot}(H_s)_2$ at the surface. As described above, the effective concentration, $C_{eff,max}$, is only involved in the calculation of the concentration of $G{\cdot}(H_s)_2$ from the one of $G{\cdot}H_s$. The total host concentration, $[H_s]_{tot}$, was calculated from eq 9 to be 6.9×10^{-8} M ($\Gamma_s = 7.9 \times 10^{-11}$ mol cm^{-2}, $A_s = 0.7$ cm^2, and $V = 0.8$ mL).[55,60] In each separate titration, the total

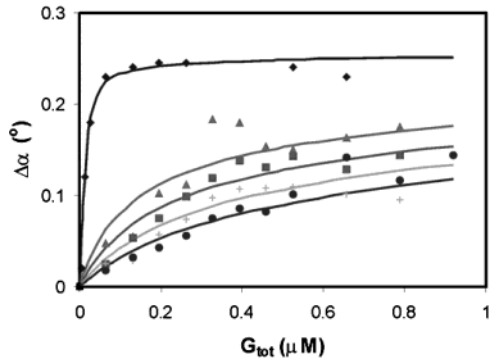

Figure 3. Experimental (markers) and calculated (lines) SPR curves for titrations of **2a** (= G) to SAMs of **1b** (H_s) in aqueous solutions of **1a** (H_l; 0.1, 0.5, 1.0, 2.5, and 5.0 mM from top to bottom, respectively). Calculated lines were produced using the multivalency model and the parameters given in Table 1.

Table 1. Optimized $K_{i,s}$ and K_{LM} Values and Corresponding Correlation Factors, R, for the Datasets Shown in Figure 3 Obtained for SPR Titrations of **2a** to SAMs of **1b** (H_s) in Aqueous Solutions of **1a** (H_l)

$[H_l]_{tot}$ (mM)	$K_{i,s}$ (M^{-1})[a]	R	K_{LM} (M^{-1})[b]	R
0.1	3.3×10^5	0.99	1.7×10^{10}	0.97
0.5	1.1×10^5	0.93	2.8×10^9	0.94
1	1.6×10^5	0.97	6.4×10^9	0.97
2.5	2.8×10^5	0.94	2.8×10^{10}	0.93
5	5.5×10^5	0.97	7.9×10^{10}	0.98

[a] Determined using the multivalency model with $n = p_{max} = 2$, $C_{eff,max} = 0.2$ M, $K_{i,l} = 4.6 \times 10^4$ M^{-1}, and $\Delta\alpha_{max} = 0.521°$. [b] Determined using a Langmuir model ($n = 2$, $p_{max} = 1$, $[H_s]_{tot} = 0.5 \times [\mathbf{1b}]_{tot}$, and for $G{\cdot}H_s{\cdot}H_l$: $K = 0$) using $K_{i,l} = 4.6 \times 10^4$ M^{-1} and $\Delta\alpha_{max} = 0.245°$, respectively; $\Delta\alpha_{max}$ values were optimized for all datasets combined.

guest concentration, $[G]_{tot}$, was varied while the total concentration of **1a** in solution, $[H_l]_{tot}$, was kept constant and was varied only from titration to titration (Figure 3). In fitting the experimental SPR data to this model, $K_{i,s}$ was optimized in the numerical routine as outlined above.

When fitting the SPR data obtained for the binding of **2a** to SAMs of **1b** in the presence of various concentrations of **1a** in solution (Figure 3), separately optimized $K_{i,s}$ values were obtained for each $[H_s]_{tot}$ value (Table 1). The overall fit of all datasets did not improve significantly when $\Delta\alpha_{max}$ was varied independently for each dataset. Therefore, one value of $\Delta\alpha_{max}$ was used as a fit parameter for all datasets. Within experimental error, these $K_{i,s}$ values were identical and amounted to log $K_{i,s} = 5.4 \pm 0.3$. In contrast, when using a Langmuir type model (assuming 1:1 binding to surface-confined dimeric CD host sites in addition to 1:1 and 1:2 complexes to CD in solution), K values spanned a wider range of a factor 30 (log $K_{LM} = 10.2 \pm 0.6$). More importantly, the Langmuir model does not allow a clear-cut comparison either to the observed stability constant of **2a** with a CD dimer in solution ($K_{1:1} = 1.2 \times 10^7$ M^{-1})[49] or to the stability of an individual Ad-CD interaction ($K_{i,l} = 4.6 \times 10^4$ M^{-1}).

The calculations using the multivalency model showed that, regardless of $[H_l]_{tot}$, the only major surface species (>99% of all surface-attached guest species) is $G{\cdot}(H_s)_2$, which is the species with the maximum number of interactions (p_{max}) to the host SAM. From simulations, it became clear that this is a normal observation when $K_{i,s}C_{eff,max} \gg 1$ and $C_{eff} = C_{eff,max}\theta_f \gg [H_l]_{tot}$. It can be intuitively understood by noting that competition between surface and solution host sites for binding a free guest site of a guest species already bound to the surface through another guest site is in favor of H_s when its concentration experienced by the guest site (i.e. C_{eff}) is larger than that of the competing H_l ($[H_l]_{tot}$). In our case, using CD complexes of the relatively small guest molecules discussed here, the condition $C_{eff} \gg [H_l]_{tot}$ usually holds for all coverages $\theta_b <$ 90% since the solubility of **1a** in water is only about 12 mM. In general, this allows simplification of the model by neglecting all surface species for which $p < p_{max}$, so that only surface species $G{\cdot}(H_s)_{p-max}{\cdot}(H_l)_q$ (for $q = 0..(n\text{-}p_{max})$) are incorporated.

The dependence of the optimized $K_{i,s}$ value on the model parameter $C_{eff,max}$ is only moderate. It appears to follow an inverse square root dependence so that changing $C_{eff,max}$ between 0.05 and 0.8 M (factor 4 lower or higher than the estimated 0.2 M, and clearly spanning all possible linker lengths and host lattice effects observable in Figure 2) leads only to changes in optimized $K_{i,s}$ values of a factor 2, which is within experimental error (see Table 1). The inverse square root relationship between $K_{i,s}$ and $C_{eff,max}$ can be understood when taking into account that $G{\cdot}(H_s)_2$ is the only major surface species as discussed above. More in general, eq 21 (for $q = 0..(n\text{-}p_{max})$) follows from the facts that $K_{i,s}$ is used to describe all (total number: p_{max}) sequential binding steps of guest sites to surface host sites (eqs 5 and 6) and that all but the first step incorporate $C_{eff,max}$ (eq 6).

$$[G{\cdot}(H_s)_{p_{max}}{\cdot}(H_l)_q] = bK_{i,s}^{p_{max}} C_{eff,max}^{(p_{max}-1)} \qquad (21)$$

In eqn 21, b is a scaling factor incorporating statistical factors determined by n, p_{max}, and q (as follows from eqs 5−8), θ_f, and terms related to the binding of H_l. It follows from eq 21 that when another $C_{eff,max}$ value is assumed, this leads to a change in the optimized $K_{i,s}$ value with a dependence of $C_{eff,max}^{-x}$ with $x = (p_{max} - 1)/p_{max}$. When $p_{max} = 2$, as is the case for **2a**, then this dependence is $C_{eff,max}^{-1/2}$, as observed above, while for large p_{max}, $K_{i,s}$ scales with $C_{eff,max}^{-1}$.

The average $K_{i,s}$ value (2.5×10^5 M^{-1}) is close to the intrinsic stability constant in solution, $K_{i,l}$. It confirms that an interaction strength of an individual Ad-CD interaction at the surface is approximately the same as in solution, as was already observed for monovalent guests.[59] Additional contributions, such as resulting from interactions between the linkers within the guest molecule and the OH groups of the rims of the host molecules, may account for the, relatively small, difference between $K_{i,s}$ and $K_{i,l}$. Alternatively, cooperativity could be playing a (small) role in this system. In general, in our opinion, only after such an analysis, trying to account for the multivalency effect while assuming independent binding and analyzing the quality of such a fitting procedure, one can draw conclusions about the absence or presence of cooperativity.

More important to note is the fact that the multivalency model described here is able to reproduce the experimental data for this divalent guest with a strong predictive power from only basic assumptions on molecular stoichiometry and geometry and readily accessible data on monovalent interactions in solution. This is in contrast to a standard Langmuir model, which gives completely different binding constants in solution and at surfaces (10^7 vs 10^{10} M^{-1}) and provides no clarity on how these should

(60) The values of A_s and V are dictated by our SPR setup.

be related to intrinsic binding constants. Furthermore, competition by CD in solution cannot be incorporated in the latter model in a straightforward manner, while the multivalency model is based on intrinsic interactions and, therefore, clearly describes the observed competition behavior (Figure 3) well.

Recently, we have obtained preliminary results with a similar guest molecule (**2b**) which has shorter spacers and thus a smaller linker length between the two Ad units which should result in a higher effective concentration.[61] So far, titrations[62] have been only performed at a single background concentration of **1a** (4 mM), which has resulted in $K_{i,s} = 6.7 \times 10^5$ M^{-1} when the same $C_{eff,max}$ value (0.2 M) is employed as used for the fitting of **2a**. This $K_{i,s}$ value is somewhat higher than the average, and actually higher than every separate value obtained for **2a**. It is clear that also in **2b** the linker is long enough for both Ad groups to be employed in binding, and the data seem to indicate a somewhat higher effective concentration resulting from the shorter linker length. This conclusion is, however, preliminary because of the relatively large experimental errors involved. Therefore, more work is needed on systematic variations of the linker length in order to fully elucidate its effect on binding parameters.

Determination of the Binding Stoichiometry at the Surface, p_{max}. Most studies related to multivalent host−guest studies focus on determining the interaction strength between host and guest, presuming the number of interactions are constant and known, and try to interpret data in terms of, for example, effective concentration or cooperativity. Alternatively, systems for which the individual interaction strength is known, but the number of interactions is not, can be worthwhile studying. In particular when dealing with surface-confined hosts (or guests), the determination of the binding stoichiometry by experimental means can be difficult to impossible, although it could potentially provide information on various issues such as how many surface host sites can sterically be reached by the multivalent guest, what influence has the surface confinement on the binding characteristics when compared to more flexible solution systems, etc.. Here, we will discuss a method to derive binding stoichiometries from stability measurement data which is applicable to multivalent guest molecules of which the intrinsic binding constant $K_{i,s}$ is known from independent measurements.

As illustrative examples, we have employed the host−guest binding of the ferrocenyl- (Fc-) functionalized poly(propylene imine) dendrimers **3a** and **3b**, which are generation-1 (with 4 Fc endgroups) and generation-2 (with 8 Fc endgroups) dendrimers, respectively, with CD SAMs. These dendrimers have been prepared before, and the binding of the Fc endgroups with CD (**1a**) in solution has been studied.[63] It was concluded that neither positive nor negative cooperativity plays a role, and a $K_{i,l}$ value of 1.2×10^3 M^{-1} was found. Their behavior in solution most likely strongly resembles the Ad-functionalized dendrimers for which it was concluded that for dendrimer generations 1−4 all (4−32) endgroups are available for complexation.[64] Furthermore, it has been shown before that the binding constants of small, univalent Fc guests closely resemble the binding constants found in solution for binding to **1a**.[59] Therefore, $K_{i,s}$ for **3a** and **3b** can be assumed to be close or equal to $K_{i,l}$ (1.2×10^3 M^{-1}). However, because of their spherical nature, their relatively small sizes, and relative rigidity,[64] it is safe to assume that not all endgroups can be involved in binding to surface host sites when such dendrimers are brought into contact with CD SAMs (of **1b**), so: $p_{max} < n$. It is, however, as also discussed above, safe to assume that *only* the species interacting with the maximum number of interactions, p_{max}, to the surface will play a major role, as experimental conditions can be easily chosen such that $C_{eff} \gg [H_l]_{tot}$.

Similarly as discussed above for **2a**, $C_{eff,max}$ for **3a** and **3b** (here employed: 0.3 M) can be estimated from linker lengths between unbound and bound Fc endgroups. Here we assume that all endgroups experience the same effective concentration and that the presence of other unbound endgroups does not influence $C_{eff,max}$. The latter can be made plausible by envisioning that a part of the molecule that will block a guest site from part of the host surface will lead to a smaller number of accessible cavities but also to a reduced probing volume, supposedly to the same extent, thus counteracting their influences on $C_{eff,max}$. This is a fairly crude approximation, but it has been argued above that fairly large changes in linker lengths lead only to minor changes in $C_{eff,max}$ (at least for disordered lattices; see Figure 2) and that fairly large changes in $C_{eff,max}$ (far outside of a range of linker lengths that can be found acceptable based on molecular modeling) lead only to marginal differences in optimized $K_{i,s}$ values, often within experimental error. In other words, the model is rather insensitive to the absolute value of $C_{eff,max}$.

Similar to the SPR experiments of **2a** as described above, titrations of **3a** and **3b** were performed at constant concentrations of competing host **1a** in solution while varying the concentration of guest (**3a** or **3b**).[62] Typical examples of such titrations are shown in Figure 4. Fitting of the data to the multivalency model was performed as described above optimizing $K_{i,s}$ but now for different values of p_{max}. The most interesting fitting solutions are given in Table 2. The fit quality was not affected for either guest when varying p_{max}, but obviously, the optimized parameter $K_{i,s}$ was different in every case. As observed above for **2a**, the calculations confirmed that the species with p_{max} interactions to the surface was the only major surface-attached guest species present under the conditions employed here.

When comparing the $K_{i,s}$ values of Table 2 to the solution estimate of $K_{i,l}$ (1.2×10^3 M^{-1}), it is clear that only sensible $K_{i,s}$ values are obtained when $p_{max} = 2$ for **3a** and $p_{max} = 3$ for **3b**. In other words, of the generation-1 dendrimer **3a**, two of the four endgroups interact with surface sites, while three of the eight endgroups present at the larger dendrimer **3b** interact with the host surface. From the sizes of the dendrimers in their maximally extended conformations (diameters of 2.4 and 2.9 nm for **3a** and **3b**, respectively) and their comparison to the periodicity of the host lattice (1.8 nm), the observed binding stoichiometries are fully understandable.[65] Only recently,[66] we have been able to obtain additional experimental proof of these binding stoichiometries by quantitatively comparing the ferrocene coverages determined by cyclic voltammetry with the

(61) Ludden, M. W. J.; Sartori, A.; Casnati, A.; Ungaro, R.; Huskens, J.; Reinhoudt, D. N. Unpublished results.
(62) SPR titrations for **2b**, **3a**, and **3b** were performed using the same equipment and the same methodology as described for **2a** (see ref 49) and earlier data (refs 48 and 59).
(63) Castro, R.; Cuardo, I.; Alonso, B.; Casado, C. M.; Morán, M.; Kaifer, A. E. *J. Am. Chem. Soc.* **1997**, *119*, 5760−5761.
(64) Michels, J. J.; Baars, M. W. P. L.; Meijer, E. W.; Huskens, J.; Reinhoudt, D. N. *J. Chem. Soc., Perkin Trans. 2* **2000**, 1914−1918.

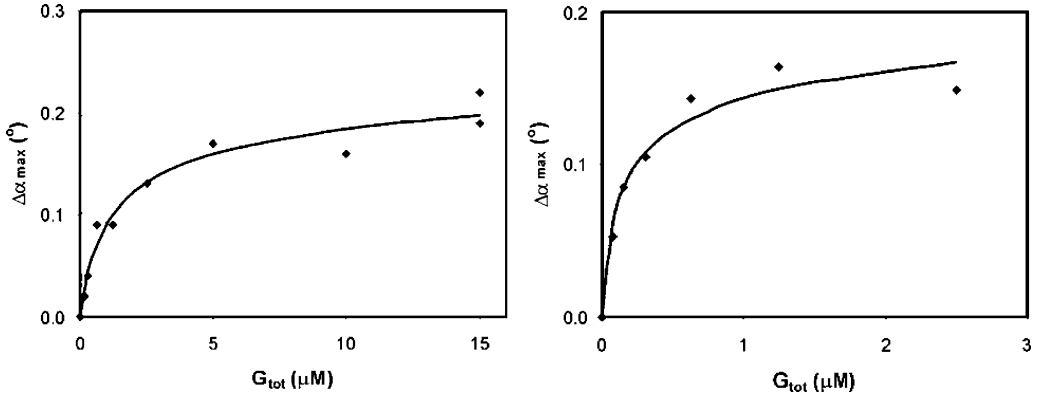

Figure 4. Experimental (markers) and calculated (lines) SPR curves for typical titrations of **3a** (left) and **3b** (right) (= G) to SAMs of **1b** (H_s) in aqueous solutions of **1a** (H_l; 0.11 mM for **3a**, 10.0 mM for **3b**). Calculated lines were produced using the multivalency model with $n = 4$, $p_{max} = 2$ for **3a** and $n = 8$, $p_{max} = 3$ for **3b**, and the parameters given in Table 2.

Table 2. Optimized $K_{i,s}$ Values for the Datasets Shown in Figure 4 for SPR Titrations of **3a** and **3b** to SAMs of **1b** (H_s) in Aqueous Solutions of **1a** (H_l)

	p_{max}	$K_{i,s}$ (M^{-1})[a]	$\Delta\alpha_{max}$ (deg)[a]	R
3a	1	2.2×10^5	0.209	0.98
	2	5.5×10^2	0.515	0.98
	3	1.0×10^2	0.886	0.98
3b	2	9.4×10^3	0.410	0.98
	3	1.1×10^3	0.715	0.98
	4	4.4×10^2	1.053	0.98

[a] Determined using the multivalency model with $n = 4$, $[H_l]_{tot} = 0.11$ mM (**3a**) or $n = 8$, $[H_l]_{tot} = 10.0$ mM (**3b**), $C_{eff,max} = 0.3$ M, and $K_{i,l} = 1.2 \times 10^3$ M^{-1}, for varying p_{max}.

surface host coverages of the CD SAMs. These exactly confirmed the stoichiometries 2 and 3 for **3a** and **3b**, respectively.

Expansion of the Model to the Prediction of Dissociation Kinetics. As noted before,[23] multivalent systems not only have a characteristic thermodynamic behavior but also show a markedly different (dissociation) kinetics when compared to monovalent systems. The association rate is, analogous to monovalent systems, determined by the diffusion of the interacting species and the intrinsic association rate constant of a monovalent interaction. The overall dissociation rate, however, is determined by the dissociation rate of the one interaction of a species in which a polyvalent guest is bound to a polyvalent host through one monovalent interaction only. The rate constant of this dissociation step can be assumed to be equal to the intrinsic dissociation rate constant of the equivalent monovalent interaction, and therefore the characteristic multivalent nature of the dissociation rate is caused solely by the dependence of the *concentration* of this species on the number of interactions, geometry of the complex, competition by and concentrations of monovalent hosts and/or guests, etc..

The same reasoning can be held for the surface systems discussed here. The association rate is simply determined by a multivalent guest from solution binding with the first site to a surface-attached host (Scheme 1, from first to second row), and thus the association rate constant to be observed for a multivalent system (in the absence of monovalent competitor in solution) is predicted to be $k_{a,obs} = nk_{a,i}$. The dissociation (Scheme 1, from second to first row) is more complex, and the model described above allows a numerical evaluation (according to eq 12) of the concentration, $[G]_{s,1}$, of the guest species, $G\cdot(H_s)\cdot(H_l)_q$ ($q = 1..(n-1)$), attached to the surface through only one interaction. The observed dissociation rate constant, $k_{d,obs}$, can then be assumed to be equal to $f_{s,1}k_{d,i}$, in which $f_{s,1}$ is the fraction of guest attached to the surface through only one interaction and $k_{d,i}$ is the intrinsic dissociation rate constant. Three limiting cases will be discussed for the dissociation of guest molecules: (A) at infinitely low surface coverages ($\theta_b = 0$) in the absence of competition; (B) as a function of surface coverage in the absence of competition; (C) as a function of the concentration of monovalent host in solution (competition) at infinitely low surface coverages.

Case A constitutes the slowest possible dissociation rate, at which $C_{eff} = C_{eff,max}$ and all guest species are bound to the surface with the maximum number of interactions, p_{max} (assuming that $K_{i,s}C_{eff,max} \gg 1$). In the special case that $n = p_{max}$,[67] the concentration of this guest species is given by eq 22 (as calculated from eqs 6−8, analogous to eq 21).

$$[G\cdot(H_s)_n] = K_{i,s}^n[G][H_s]C_{eff,max}^{(n-1)}\theta_f^{(n-1)} \qquad (22)$$

Thus, the fraction of guest bound by a single interaction, $f_{s,1}$, is given by eq 23 when substituting eqs 22 and 5 into eq 13 and when noting that $[G]_s = [G\cdot(H_s)_n]$:

$$f_{s,1} = \frac{[G]_{s,1}}{[G]_s} = \frac{n}{(K_{i,s}C_{eff,max}\theta_f)^{n-1}} \qquad (23)$$

In the limiting case that $\theta_f = 1$, this can be simplified further, and $k_{d,obs}$ is given by eq 24.

(65) For dendrimer **3a**, there may be an additional effect playing a role: from molecular modeling, it seems improbable that a Fc endgroup from a dendritic branch of which another Fc group is already attached to a host site is able to reach a neighboring CD cavity. This can offer an alternative explanation for the observed stoichiometry (2) since **3a** has only two dendritic branches, and it also, in part, explains the somewhat lower $K_{i,s}$ value observed for **3a** (Table 2, $p_{max} = 2$) compared to $K_{i,l}$ because then the model should in fact be altered to incorporate the effect that, upon binding of the second Fc group, only two Fc groups are available for binding instead of three. Incorporation of this effect, only resulting in a change of the prefactor in eq 6, results in $K_{i,s} = 6.7 \times 10^2$ M^{-1}. In principle, the same reasoning can be held for the larger dendrimers such as **3b**, but its effect on both stoichiometry and binding affinity becomes negligible, since the number of dendritic arms in these cases is always larger than the number of accessible surface sites when solely judged on molecular sizes, and the change of the prefactor in eq 6 is only marginal.

(66) Nijhuis, C. A.; Huskens, J.; Reinhoudt, D. N. *J. Am. Chem. Soc.*, submitted.

(67) For $p_{max} < n$, an analogous expression can be derived which contains an extra prefactor determined by statistical factors as given in eqs 5 and 6.

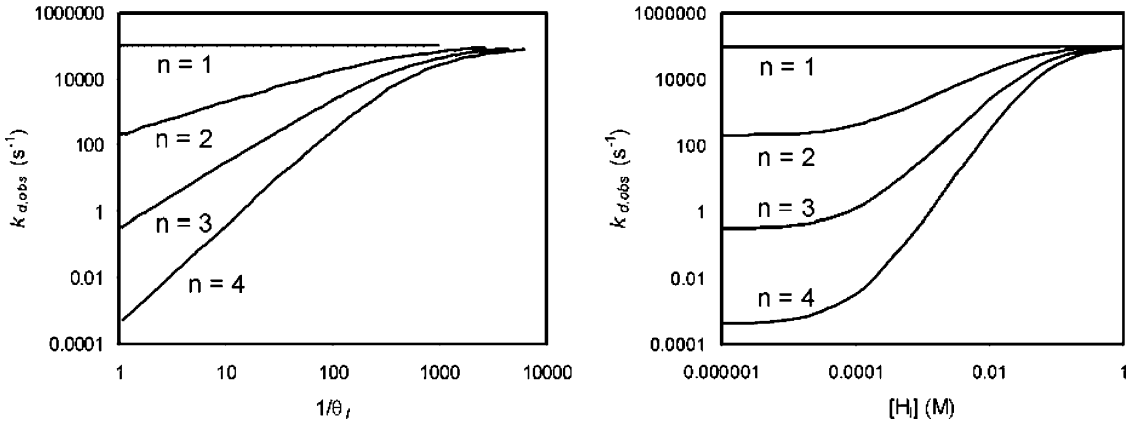

Figure 5. Simulation (using $C_{eff,max} = 0.1$ M, $\Gamma_s = 6.0 \times 10^{-11}$ mol cm^{-2}, $K_{i,s} = K_{i,l} = 10^4$ M^{-1}, $k_{a,i} = 10^9$ M^{-1} s^{-1}, $k_{d,i} = 10^5$ s^{-1}) of observed dissociation rate constants, $k_{d,obs}$, as a function of $1/\theta_f$ ((left) case B: surface coverage dependence; $[H_l]_{tot} = 0$; $[G]_{tot}$ is varied from 10^{-9} to 10^{-1} M) and as a function of $[H_l]$ ((right) case C: in competition with a host in solution; $[G]_{tot} = 10^{-10}$ M: $\theta_f > 0.99$) for varying numbers of interactions n ($= p_{max}$).

$$k_{d,obs} = f_{s,1}k_{d,i} = \frac{n}{(K_{i,s}C_{eff,max})^{n-1}}k_{d,i} \qquad (24)$$

Here it is seen that the (maximal) dissociation rate decrease (compared to the monovalent case) is determined by the number of interactions, n, and the dimensionless parameter $K_{i,s}C_{eff,max}$.

In case B, in which $\theta_f < 1$, the dependence of the observed rate constant, $k_{d,obs}$, is more complex. For (fairly high) values of θ_f for which the only major surface species is still G·$(H_s)_n$ (with $n = p_{max}$), this dependence is given by eqs 22 and 23. At the other extreme, for $\theta_f = 0$, G·H_s is the only surface species, and $k_{d,obs} = k_{d,i}$. Between, the dependence of $k_{d,obs}$ can be determined numerically, as shown graphically in Figure 5 (left). This graph shows case A as the limiting values for $1/\theta_f = 1$. The dependence at fairly high θ_f (low $1/\theta_f$) is linear (for the given plot of log $k_{d,obs}$ vs log($1/\theta_f$)) as predicted by eq 23. Also the slope of (n-1) is shown clearly. For low θ_f (high $1/\theta_f$), $k_{d,obs}$ levels off to the limiting $k_{d,i}$.

In case C, when dealing with competition with a monovalent host in solution at low surface coverages, $f_{s,1}$ is given by eq 25.

$$f_{s,1} = \frac{[G]_{s,1}}{[G]_s} = \frac{[G{\cdot}H_s](1 + K_{i,l}[H_l](1 + \ldots))}{[G]_s} \qquad (25)$$

When $K_{i,l}[H_l] \gg 1$, so when the concentration of competiting monovalent host is effectively blocking all free guest sites, eq 25 can be reduced to eq 26 (still assuming that $[G]_s = [G{\cdot}(H_s)_n]$ which is valid for $K_{i,s}C_{eff,max} \gg 1$).

$$f_{s,1} = \frac{[G]_{s,1}}{[G]_s} = \frac{n(K_{i,l}[H_l])^{n-1}}{(K_{i,s}C_{eff,max}\,\theta_f)^{n-1}} \qquad (26)$$

In the limiting case that $K_{i,s} = K_{i,l}$ and $\theta_f = 1$, this can be simplified further, and $k_{d,obs}$ is given by eq 27.

$$k_{d,obs} = f_{s,1}k_{d,i} = n([H_l]/C_{eff,max})^{n-1}k_{d,i} \qquad (27)$$

Here it is seen that the dissociation rate enhancement (compared to the lowest dissociation rate, achieved at $[H_l] = 0$ and $\theta_f = 1$), valid at intermediate $[H_l]$, is determined by the number of interactions, n, and the dimensionless parameter $[H_l]/C_{eff,max}$. For the extreme cases, so (i) when $K_{i,l}[H_l] \gg 1$ is not valid, as is the case for low competitor concentrations, and (ii) when $[H_l]$ is so high that $[G]_s = [G{\cdot}(H_s)_n]$ is not valid anymore, the dependence of $k_{d,obs}$ can be determined numerically from eq 25, as shown graphically in Figure 5 (right). Like Figure 5 (left), this graph also shows case A as the limiting values for small $[H_l]$. The linear dependence of log $k_{d,obs}$ vs log($[H_l]$), as predicted by eq 27, is seen in the intermediate, approximately linear, steep parts of the sigmoidal curves, and the slopes of (n − 1) are again predicted correctly.

It should be emphasized that these simulations represent ideal, independent interactions; i.e., they do not incorporate effects of, for example, reduced accessibility of hosts from solution binding to free interaction sites of surface-attached guest molecules. Furthermore, as shown above, only microscopic dissociation rate constants have been calculated. Macroscopic, observed rate constants are often obscured by mass transport limitation, which is often expressed as rebinding. Especially for the experimental systems discussed here, which are expected to follow diffusion-limited association, this is a serious practical problem when interpreting experimental kinetic data. Nevertheless, the graphs show some general aspects to be expected for surface-attached multivalent systems.

First of all, dissociation rate constants are strongly dependent on surface coverage. Thus, for high coverages, which can already be reached with multivalent systems at low guest concentrations in solution, the dissociation rate will approximate the rate for the corresponding monovalent system. This implies, among others, that exchange of polyvalent molecules should be feasible, even though the molecules in absence of another molecule in solution bind strongly to the interface. On the other hand, when one tries to wash away molecules from an interface without competitors in solution, the surface coverage drops, but the dissociation rate drops concomitantly, thus leading to kinetically stable assemblies of which the surface coverage depends on n and $K_{i,s}$. For example, when slow kinetics is (arbitrarily) defined as $k_{d,obs} < 0.01$ s^{-1}, a surface coverage of about two-thirds is predicted to remain at the layer when $n = 4$ (for conditions used in Figure 5), but all guest is removed for smaller n. Qualitatively, this behavior has been confirmed by our experiments on molecular printboards.[49]

Second, these results show that competition with a monovalent competitor in solution accelerates dissociation, eventually, at very high competitor concentrations,[68] up to the dissociation rate of a monovalent system. Also this has been qualitatively

confirmed before.[49] More quantitative experiments should be performed in the future using for example SPR, for which models are available which are able to deconvolute contributions from microscopic dissociation and mass transport limitation. Nevertheless, the results shown here emphasize that this will have to be done with great care, as this deconvolution is usually accomplished by performing kinetics experiments at different competitor concentrations. Then it is assumed that the microscopic dissociation constant does not change, which is shown here to be not true for multivalent systems.

Multvalency versus Cooperativity. Ercolani[36] has argued convincingly that for solution systems multivalency is not to be confused with cooperativity and that traditional methods for evaluating cooperativity fail for multivalent systems. It is therefore clear that, when dealing with multivalent systems, interpretation of thermodynamic (and possibly kinetic) data has to start with assuming *independent* interactions. This can be done in two ways: (i) assuming the intrinsic stability constant equal to the value for an independently determined monovalent system and deriving effective molarity values from ratios between inter- and intramolecular equilibrium steps; (ii) estimating an effective concentration from a (simple) molecular model and deriving intrinsic stability constants from the overall stability and the effective concentration. The former has been commonly applied to divalent systems but still rarely to more complicated situations.[23,42c] The latter approach has been used for example by Lees.[21] It is clear that such approaches can and should be followed more rigorously for high-stoichiometry assemblies, which may then eventually also allow extension to and thus a more quantitative evaluation of multivalency in aggregation phenomena.

The quality of the fit, and thus a proper evaluation of the assumption of independent interactions, can only be made when the obtained effective molarities are compared to effective concentrations estimated from molecular models (former case) or when the calculated intrinsic stability constants are compared to independently determined values for monovalent systems (latter case). Both approaches are equally valid, and they allow conclusions on the absence (when EM = C_{eff} or $K_{i,s} = K_{i,l}$, respectively) or presence of cooperativity (positive cooperativity when EM > C_{eff} or $K_{i,s} > K_{i,l}$, respectively). For example, a solution system, consisting of the recognition of a tris(ammonium) derivative by a tris(crown ether) host,[69] was prematurely interpreted as a case of (positive) cooperativity. It can be shown using the effective molarity concept that EM in this case is about 0.05 M,[70] which is probably not far from an effective concentration to be estimated from a molecular model. Therefore, the assumption of independent interactions appears to hold here, and the observed binding enhancement of the trivalent system compared to the monovalent case stems solely from multivalency and not from cooperativity. Other solution systems have been similarly reevaluated as well.[36]

In earlier studies on *surface* systems, data were either described only qualitatively (sometimes necessarily when dealing with polymeric systems)[24,29d,30,33] or simply provided as overall stabilities (Langmuir fit) without attempting to interpret them to elucidate the multivalency effect[28,29a−c,32] or interpreted in terms of cooperativity only.[26,27] Interpretation in terms of cooperativity becomes especially problematic when solution and surface stability constants (with different units) are directly compared. For example, the nicely dissected stability constants for the two-step binding of a divalent receptor to surface-attached ligands has been incorrectly interpreted as positive cooperativity.[27] In fact, when employing the model described here, it can be shown that calculated EM values are unrealistically low,[71] leading to a calculated linker length L of 200 nm, much larger than the size of the receptor molecule. Therefore, the conclusion should have read *negative* cooperativity instead of positive. In another case,[25] a quantitative description of the stabilities of the various surface species with different numbers of interactions was given but without the incorporation of the effective concentration concept.

When reviewing the surface systems evaluated in the current study, the optimized $K_{i,s}$ value for the binding of **2a** to the CD SAMs is somewhat higher than the monovalent value $K_{i,l}$. This can be interpreted as positive cooperativity, possibly due to additional interactions between the calixarene platform and the rims of the surface-attached cyclodextrin cavities, or alternatively as an interface effect, stemming from e.g. changes in the dielectric constant at the interface as has been observed and theoretically supported for the hydrogen bonding to lipid membrane interfaces.[72] In contrast, from the binding constants derived for **3a** and **3b**, it is obvious that the enhanced binding compared to the binding of monovalent CD in solution can be solely attributed to multivalency in these cases.

Conclusions

Multivalency at interfaces is of high interest, since it is one of nature's governing principles in cell recognition, including the infection by viruses and bacteria. The model described here gives an insight into how multiple, independent interactions provide a collective thermodynamic and kinetic stability enhancement. The model is based on the concept of effective concentration, which allows an interpretation based on molecular structure. Some dependencies of the model on model parameters, such as the linker length, are different at interfaces than in solution. Generally, receptor densities at an interface can often be larger than can be reached in solution, while the probing volume is often smaller, resulting in significantly larger effective concentrations than present in solution systems, leading to stronger binding at interfaces than to those corresponding solution systems.

(68) Such high competitor concentrations may be impossible to reach as is for example the case for cyclodextrin where the maximal [H_l] is about 0.01 M, as it is limited by solubility.

(69) Balzani, V.; Clemente-León, M.; Credi, A.; Lowe, J. N.; Badjić, J. D.; Stoddart, J. F.; Williams, D. J. *Chem.—Eur. J.* **2003**, *9*, 5348−5360.

(70) Using the overall stability constant $K = 10^6$ M^{-1} and the intrinsic value $K_i = 420$ M^{-1} (both determined in acetonitrile; see ref 69), and the notion that, for a trivalent system, $K = 6EM^2K_i^3$, EM = 0.05 M is calculated. When using this value for the binding in chloroform ($K_i = 2.7 \times 10^4$ M^{-1}), $K = 2.5 \times 10^{11}$ M^{-1} is calculated which also agrees with their observation of $K > 10^7$ M^{-1} in this case.

(71) Using the terminology described in ref 27, the first binding step of the divalent receptor (G) to a surface-bound ligand (H_s) site is given by $K_1 = [G{\cdot}H_s]/[G][H_s] = 4 \times 10^4$ M^{-1} and the second step, defined as an intermolecular binding step with a second ligand site, by $K_2 = [G{\cdot}(H_s)_2]/[G{\cdot}H_s][H_s] = 7.3 \times 10^7$ m^2 mol^{-1}. Using the terminology and model described here, $K_1 = 2K_i$ and $K_2 = K_iEM/2\Gamma_s$. The former leads to $K_i = 2 \times 10^4$ M^{-1}, and the latter, with $\Gamma_s = 2 \times 10^{-9} - 1 \times 10^{-7}$ mol m^{-2}, leads to EM = 0.01−0.5 mM. When assuming $C_{eff,\ max}$ = EM (valid for independent binding sites, i.e., noncooperativity) and using eq 20, L = 200 nm. This is clearly much larger than the size of the receptor. Thus it can be concluded that EM < $C_{eff,\ max}$, indicating negative cooperativity.

(72) (a) Sasaki, D. Y.; Kurihara, K.; Kunitake, T. *J. Am. Chem. Soc.* **1991**, *113*, 9685−9686. (b) Sakurai, M.; Tamagawa, H.; Inoue, Y.; Ariga, K.; Kunitake, T. *J. Phys. Chem. B* **1997**, *101*, 4810−4816. (c) Tamagawa, H.; Sakurai, M.; Inoue, Y.; Ariga, K.; Kunitake, T. *J. Phys. Chem. B* **1997**, *101*, 4817−4825.

The model provides, for the first time, a tool to critically evaluate observed stability constants at interfaces. Based on the assumption of independent interactions, intrinsic stability constants are obtained which are to be compared to independently determined values for monovalent analogues. This comparison offers a fair judgment of the validity of the independency assumption and thus of the absence or presence of cooperativity, which is, until now, often put forward as the source of stability enhancement without proper arguments. Alternatively, the type of reasoning followed here may provide a way for estimating whether local changes of receptor densities occur, possibly induced by the binding of the multivalent molecule, a phenomenon often speculated upon but never supported by quantitative data.

Besides for understanding nature's design of cell recognition and for designing better drugs based on multivalency, a third reason for trying to unravel the governing principles of multivalency at interfaces is its potential for use in nanofabrication. We have shown recently that multivalent molecules can be bound in a thermodynamically and/or kinetically stable fashion at surfaces employing multiple, intrinsically weak, supramolecular interactions.[48,49] Stable patterns of such molecules have been prepared, e.g., by microcontact printing and dip-pen nanolithography, and erasing of such patterns was possible using competition with a monovalent competitor or another external stimulus, such as electrochemical oxidation.[49a] We strongly believe that multivalency can be used to a much larger extent to assemble larger architectures on surfaces, also employing for example layer-by-layer techniques, since multivalency allows an ultimate control over thermodynamic and kinetic parameters.

Acknowledgment. This research is supported by the Council for Chemical Sciences of The Netherlands Organization for Scientific Research (CW-NWO) (T.A.: Grant Number 97041. A.M.: CW-programmasubsidie 700.98.305. M.J.W.L.: Vidi Vernieuwingsimpuls Grant 700.52.423 to J.H.) and the Technology Foundation STW, applied science division of NWO and the technology program of the Ministry of Economic Affairs (C.A.N.: Project Number TST4946).

JA049085K